Electronic Supplementary Information (ESI)

A novel silver(I)-Keggin-polyoxometalate inorganic-organic hybrid: Lewis acid catalyst for cyanosilylation reaction

Tuo-Ping Hu,[a,b] Ya-Qin Zhao,[a] Kai Mei,[a] Shu-Jie Lin,[a] Xing-Po Wang,[a] and Di Sun[a,*]

a

[a]*Key Lab of Colloid and Interface Chemistry, Ministry of Education, School of Chemistry and Chemical Engineering, Shandong University, Jinan, 250100, P. R. China. E-mail: dsun@sdu.edu.cn*

[b]*Department of Chemistry, North University of China, Taiyuan, Shanxi 030051, People's Republic of China.*

.

1. Table S1. Selected bond lengths and angles for 1.

Ag1—N8	2.24 (4)	Ag3—N7	2.21 (4)
Ag1—N12^{i}	2.15 (4)	Ag3—N10	2.21 (4)
Ag1—O3^{ii}	2.83 (2)	Ag3—O1^{v}	2.73 (3)
Ag1—O23	2.88 (2)	Ag3—O13	2.81 (3)
Ag2—N1	2.24 (4)	Ag4—N3^{vi}	2.24 (4)
Ag2—N6	2.23 (4)	Ag4—N4	2.20 (4)
Ag2—O19	2.57 (4)	Ag4—O17	2.61 (2)
Ag2—O23^{iii}	2.62 (2)	Ag4—O34^{vii}	2.74 (3)
Ag2—O32^{iv}	2.65 (2)		
N8—Ag1—O3^{ii}	75.8 (11)	O19—Ag2—O32^{iv}	143.5 (7)
N8—Ag1—O23	96.0 (10)	O23^{iii}—Ag2—O32^{iv}	112.4 (6)
N12^{i}—Ag1—N8	149.0 (16)	N7—Ag3—O1^{v}	80.3 (10)
N12^{i}—Ag1—O3^{ii}	82.0 (10)	N7—Ag3—O13	107.3 (10)
N12^{i}—Ag1—O23	99.1 (9)	N7—Ag3—N10	160.8 (15)
O3^{ii}—Ag1—O23	162.7 (7)	N10—Ag3—O1^{v}	80.5 (10)
N1—Ag2—O19	105.8 (14)	N10—Ag3—O13	90.0 (10)
N1—Ag2—O23^{iii}	83.9 (9)	O1^{v}—Ag3—O13	154.5 (7)
N1—Ag2—O32^{iv}	77.7 (10)	N3^{vi}—Ag4—O17	103.2 (9)
N6—Ag2—N1	155.4 (15)	N3^{vi}—Ag4—O34^{vii}	74.1 (9)
N6—Ag2—O19	93.7 (13)	N4—Ag4—N3^{vi}	158.0 (16)
N6—Ag2—O23^{iii}	106.1 (9)	N4—Ag4—O17	93.8 (9)
N6—Ag2—O32^{iv}	77.8 (10)	N4—Ag4—O34^{vii}	90.1 (9)
O19—Ag2—O23^{iii}	104.1 (7)	O17—Ag4—O34^{vii}	174.1 (7)

Symmetry codes: (i) $x+1/2$, $-y+1$, $z-1/2$; (ii) $x+1$, y, z; (iii) $x-1/2$, $-y+1$, $z-1/2$; (iv) $x-1/2$, $-y+2$, $z-1/2$; (v) $x+1/2$, $-y+1$, $z+1/2$; (vi) $x-1/2$, $-y+2$, $z+1/2$; (vii) $x-1$, y, z.

2. Figure S1. The XRD pattern of 1.

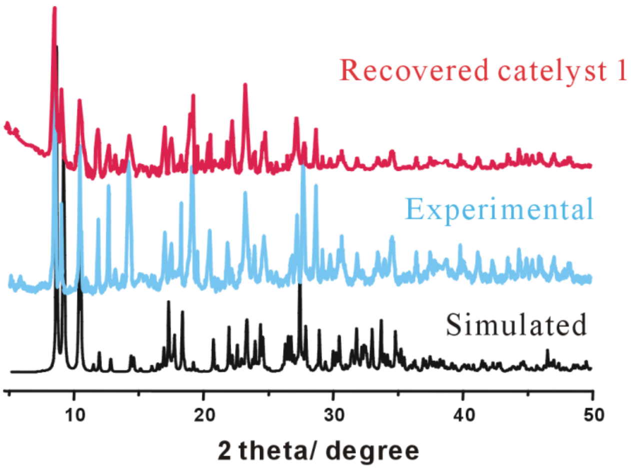

As shown in Fig. S1, the X-ray powder diffraction patterns measured for the as-synthesized sample of **1** is in good agreement with the PXRD patterns simulated from the respective single-crystal X-ray data, proving the purity of the bulk phases. The dissimilarity in reflection intensities between the simulated and the experimental patterns may be due to the different orientation of the microcrystals in the powder samples. For recovered catalyst **1**, most diffraction peaks are also well-matched with simulated ones, indicating the integrity of **1** after catalysis, some broaden peak and few slighly splitted peaks indicate somewhat distortion of the network.

3. Figure S2. The TGA for 1.

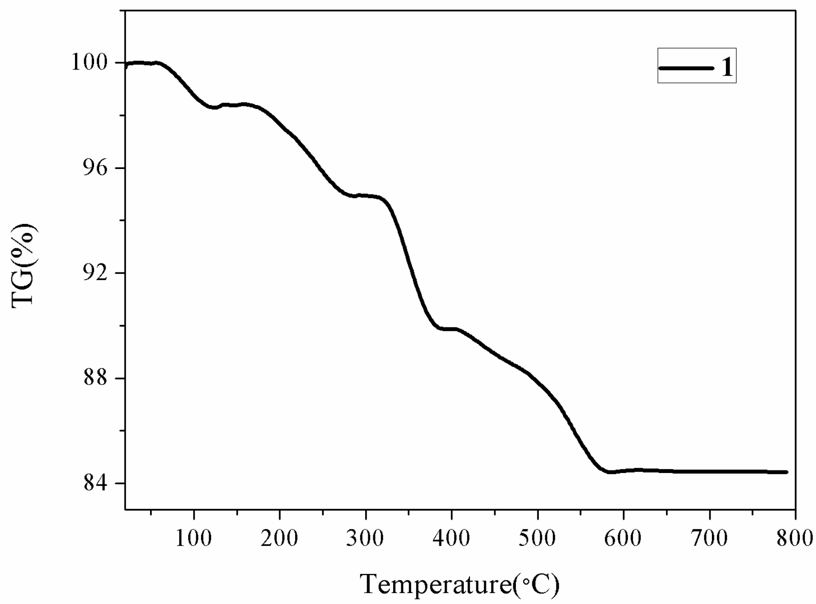

4. Figure S3. The IR for 1.

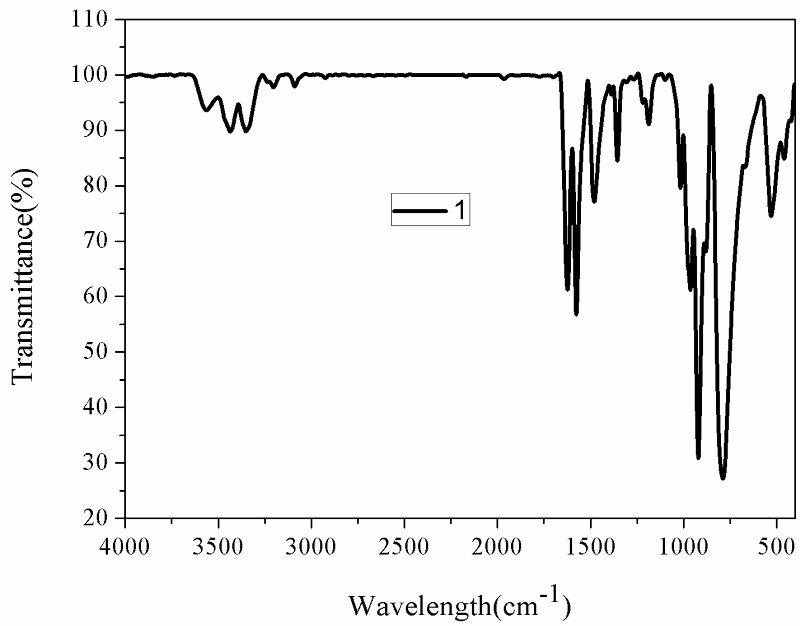

5. Figure S4 ^{1}H NMR spectra for reaction mixtures after catalysis by 1.

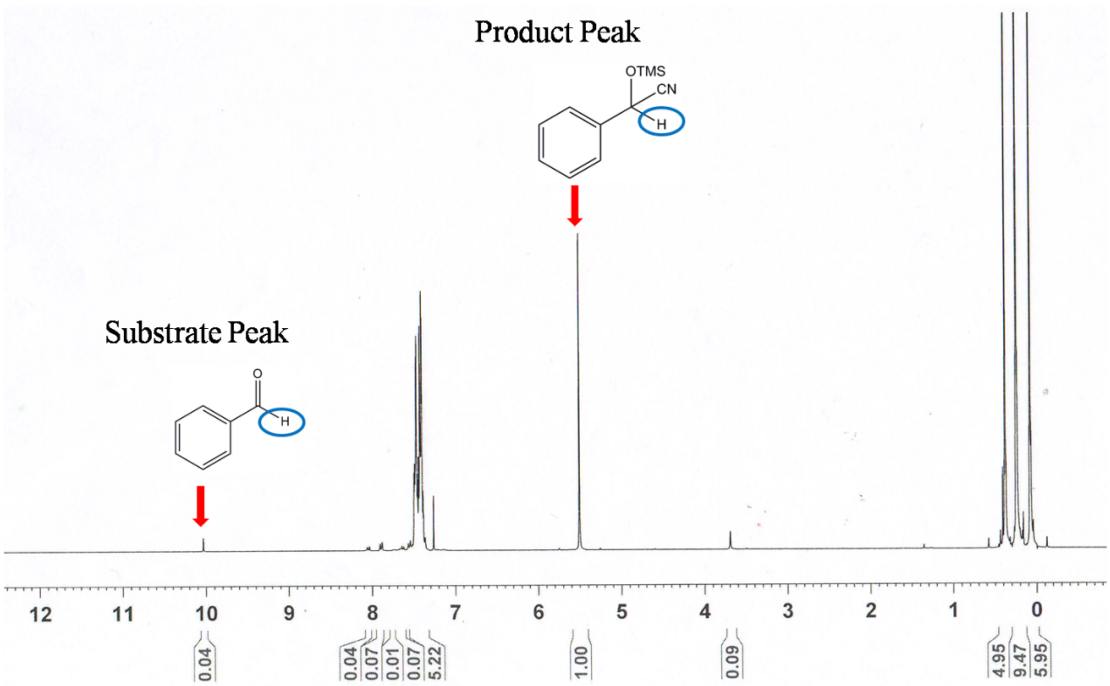

(a) ^{1}H NMR of crude reaction mixture corresponding to Table1, entry 1.

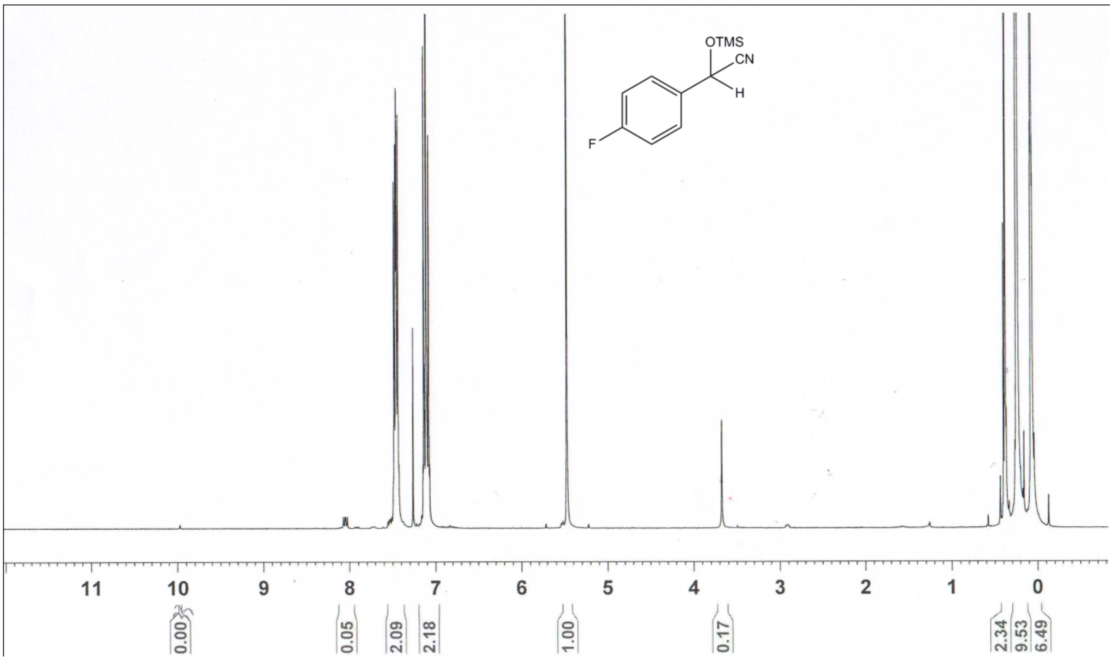

(b) ^{1}H NMR of crude reaction mixture corresponding to Table1, entry 2.

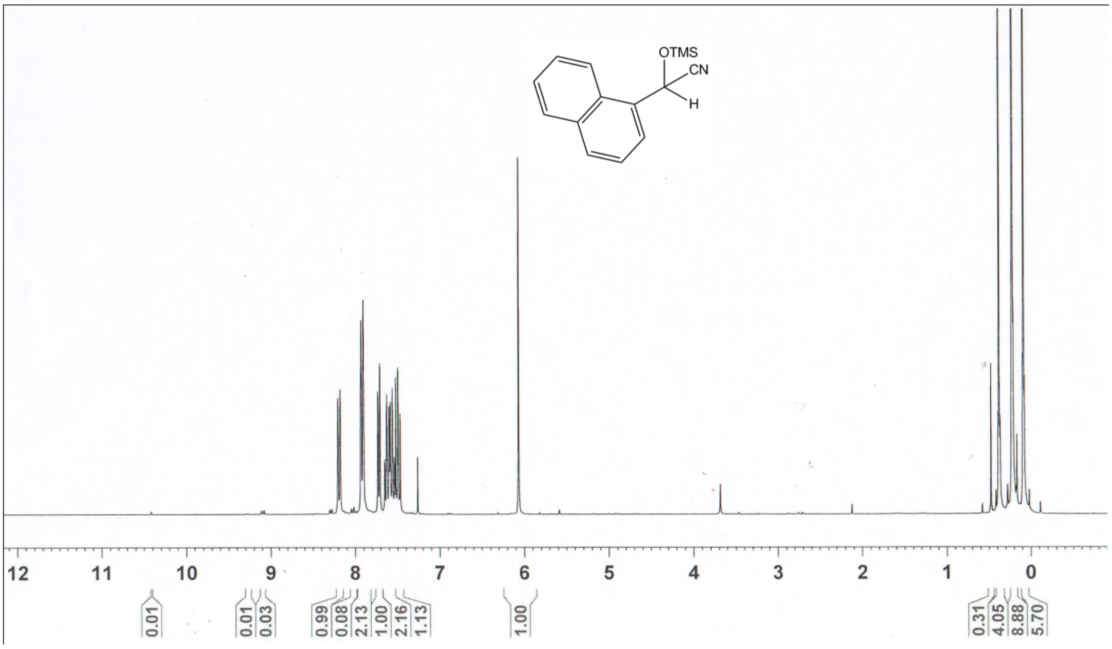

(c) [1]H NMR of crude reaction mixture corresponding to Table1, entry 3.

(d) [1]H NMR of crude reaction mixture corresponding to Table1, entry 4.

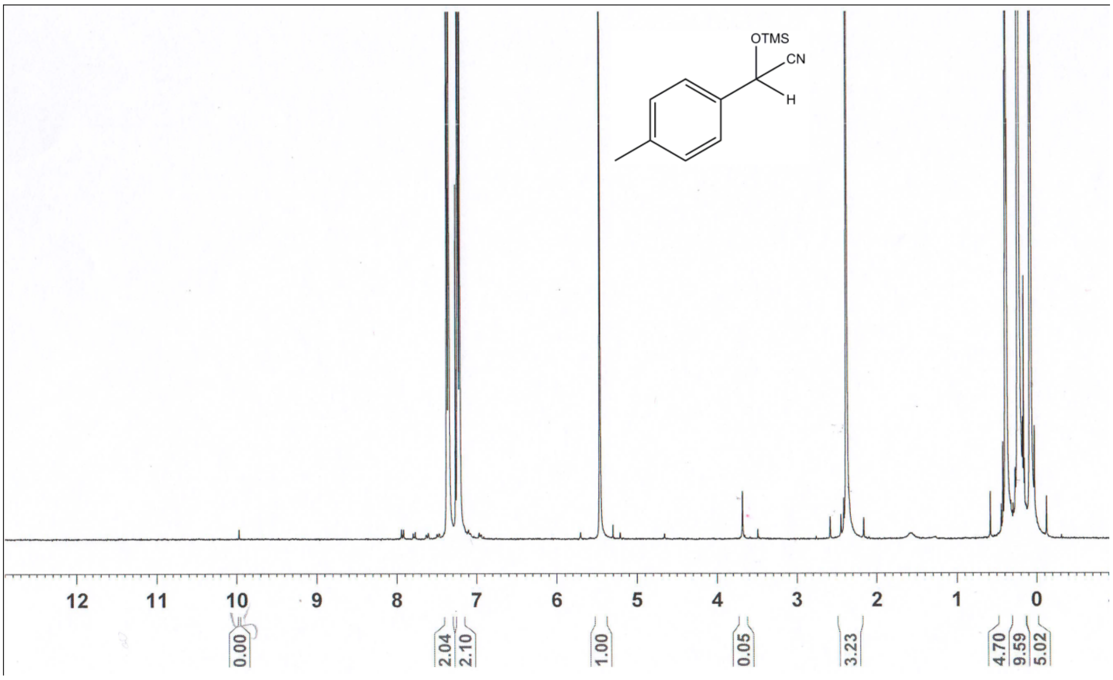

(e) [1]H NMR of crude reaction mixture corresponding to Table1, entry 5.

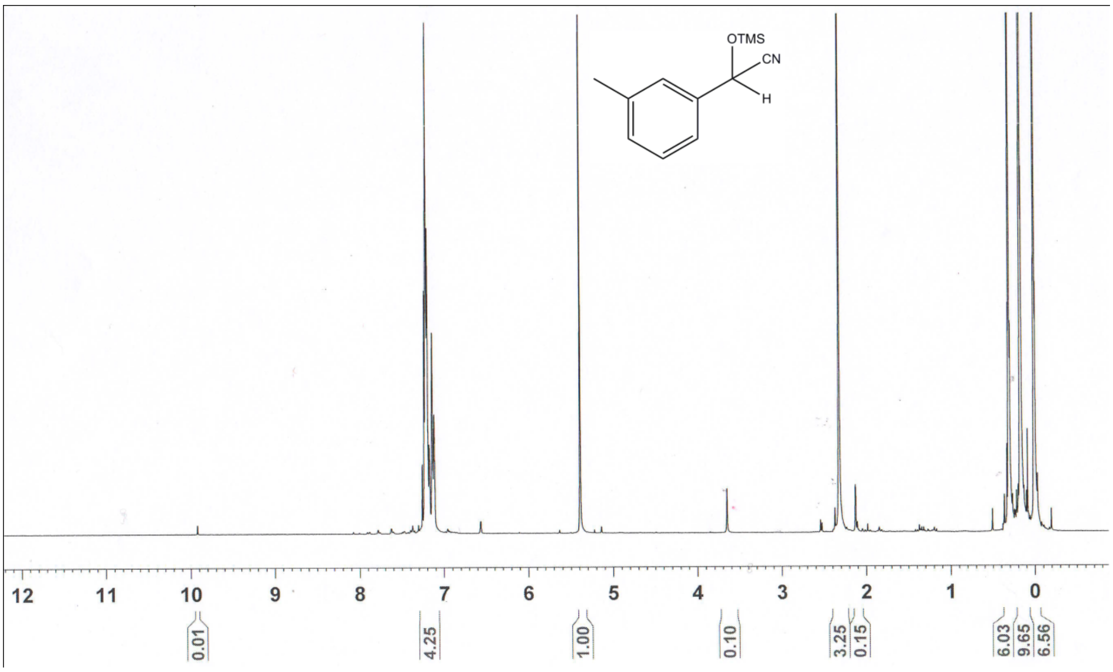

(f) [1]H NMR of crude reaction mixture corresponding to Table1, entry 6.

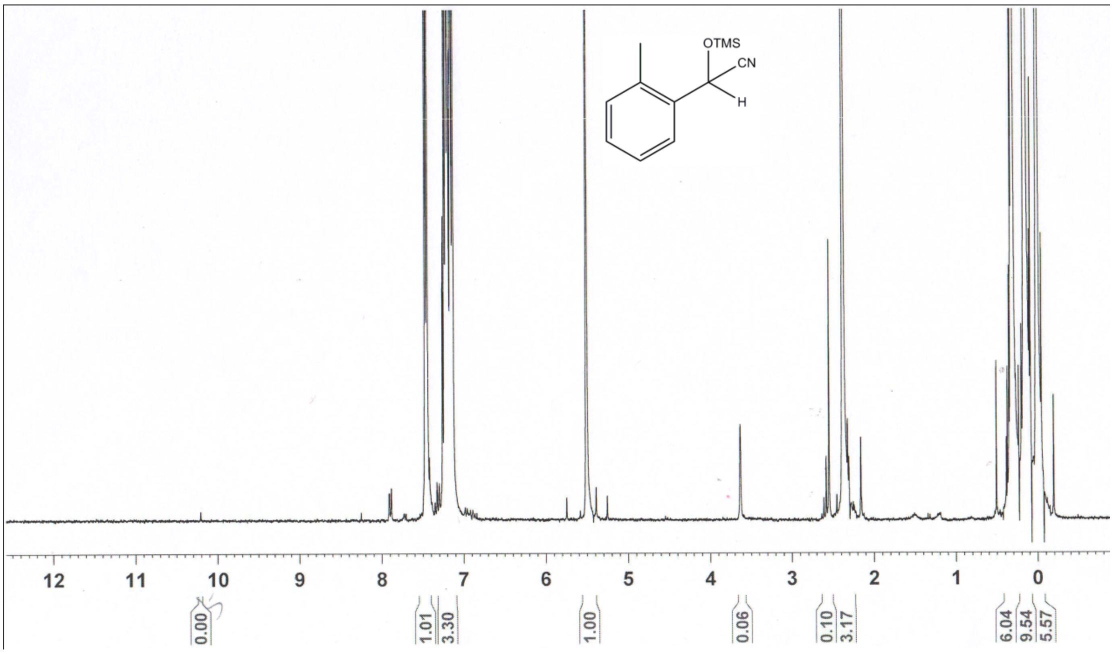

(g) [1]H NMR of crude reaction mixture corresponding to Table1, entry 7.

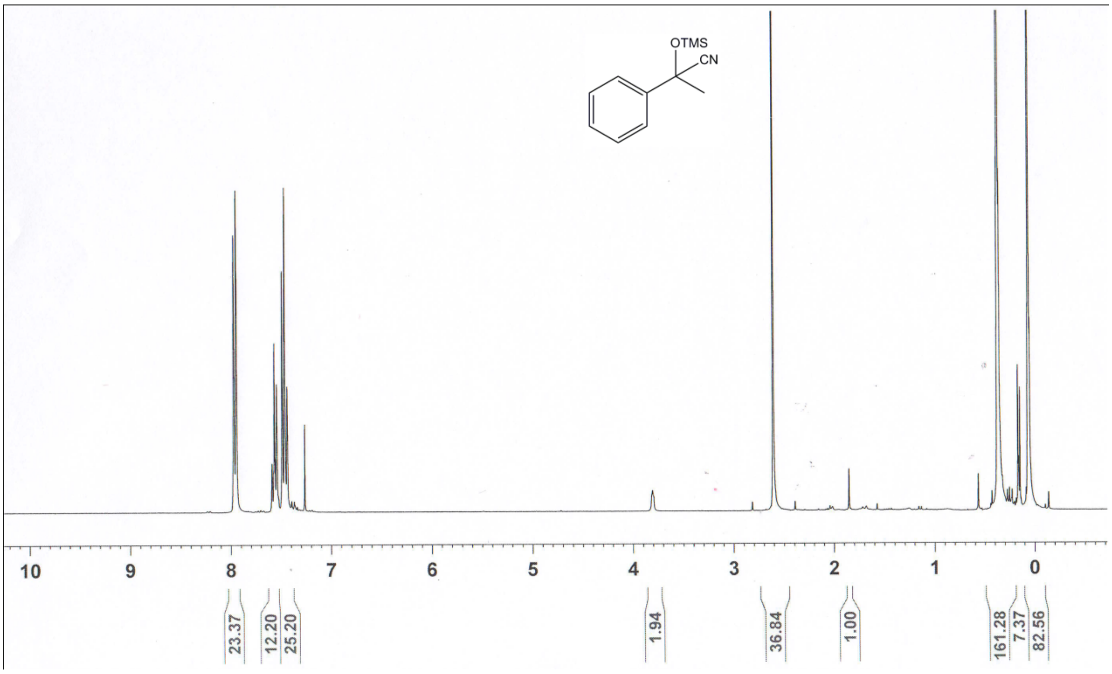

(h) [1]H NMR of crude reaction mixture corresponding to Table1, entry 8.

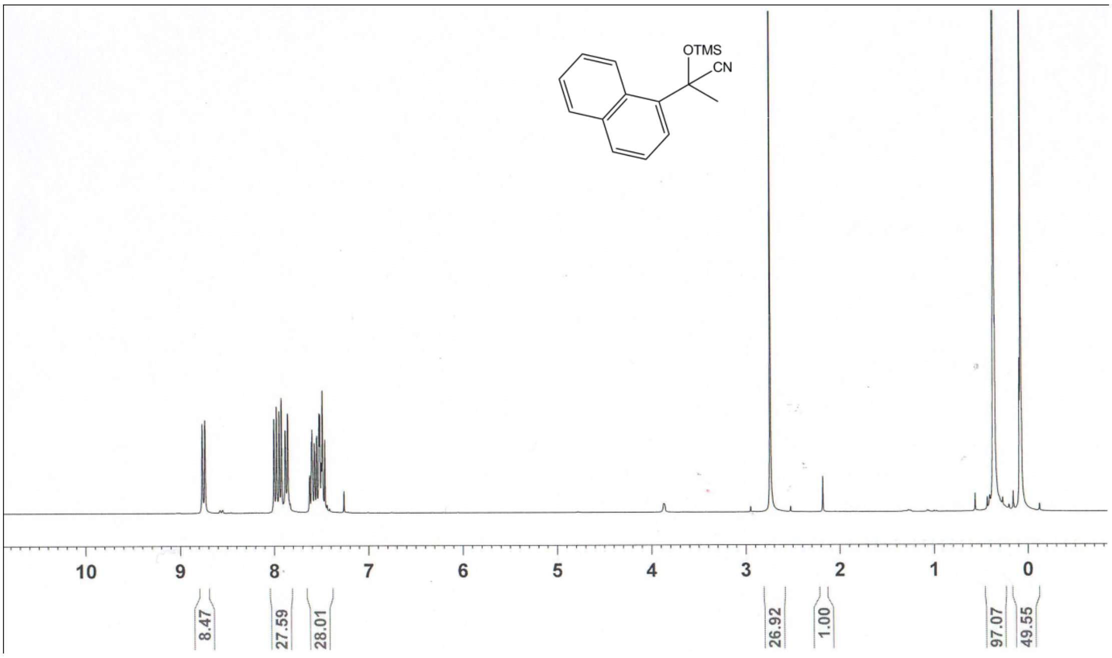

(i) ¹H NMR of crude reaction mixture corresponding to Table1, entry 9.

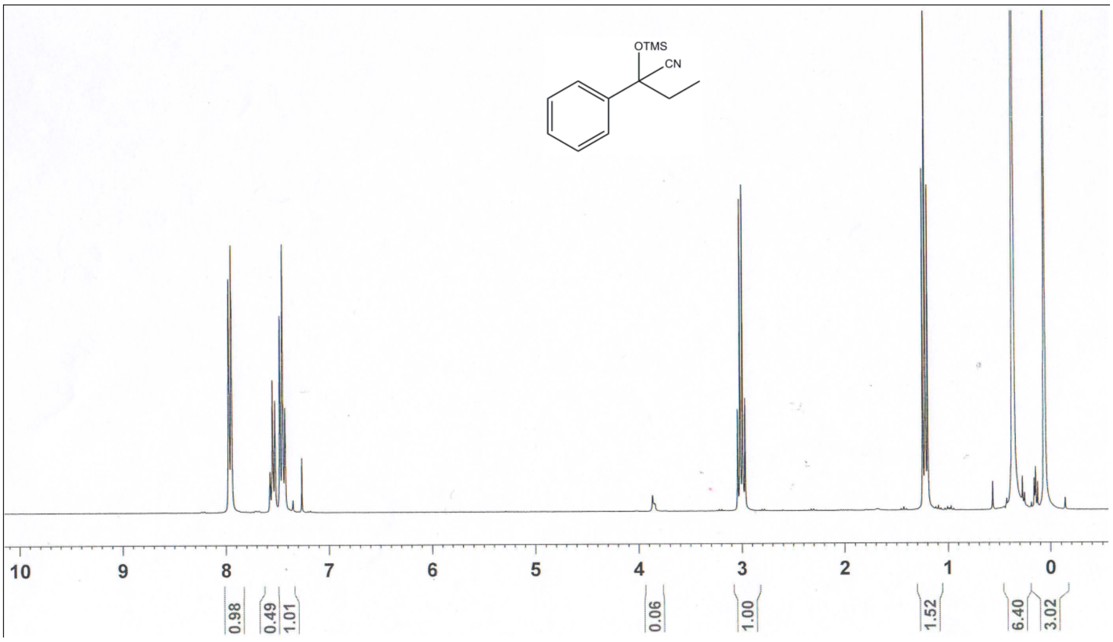

(j) ¹H NMR of crude reaction mixture corresponding to Table1, entry 10.

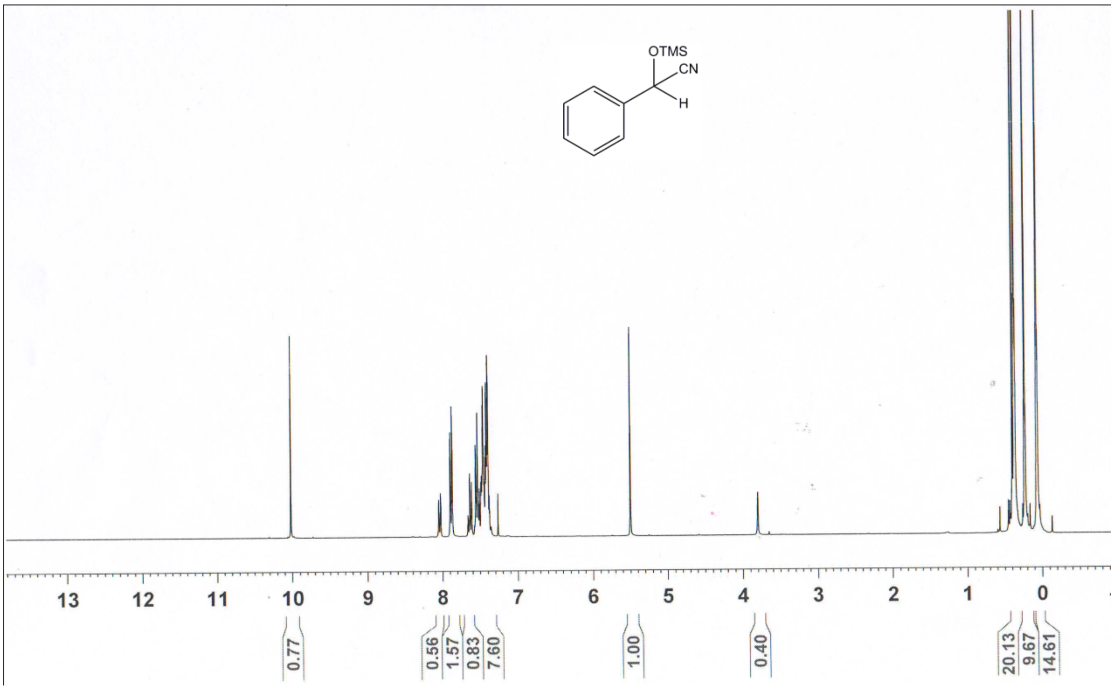

(k) ^{1}H NMR of crude reaction mixture corresponding to Table2, entry 1.

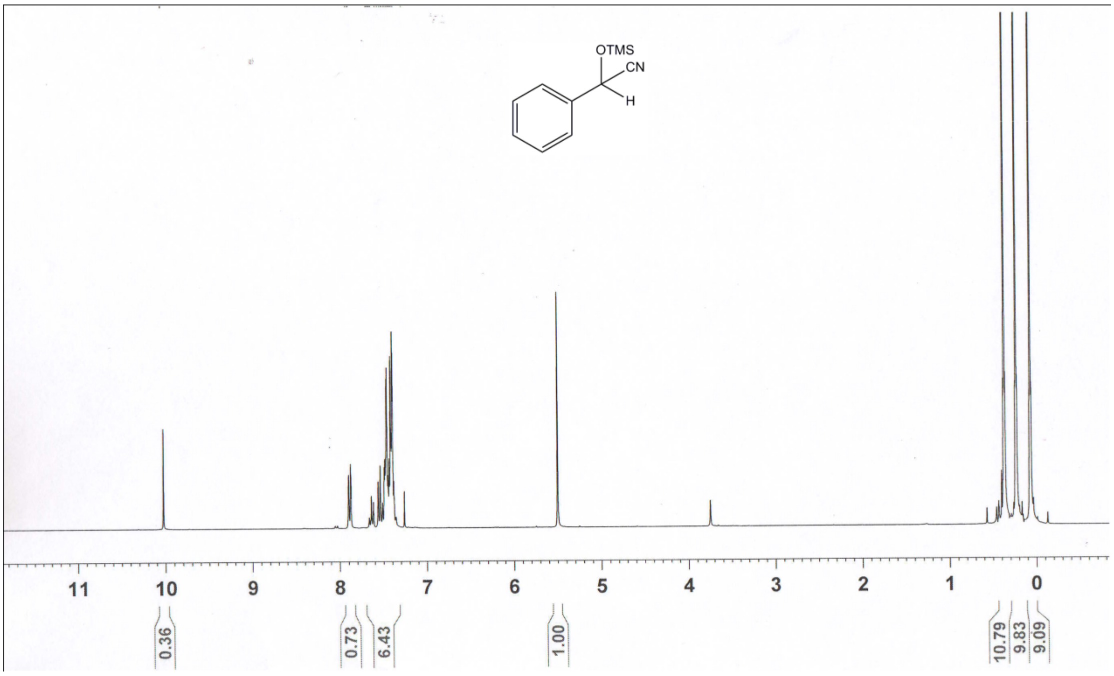

(l) ^{1}H NMR of crude reaction mixture corresponding to Table2, entry 2.

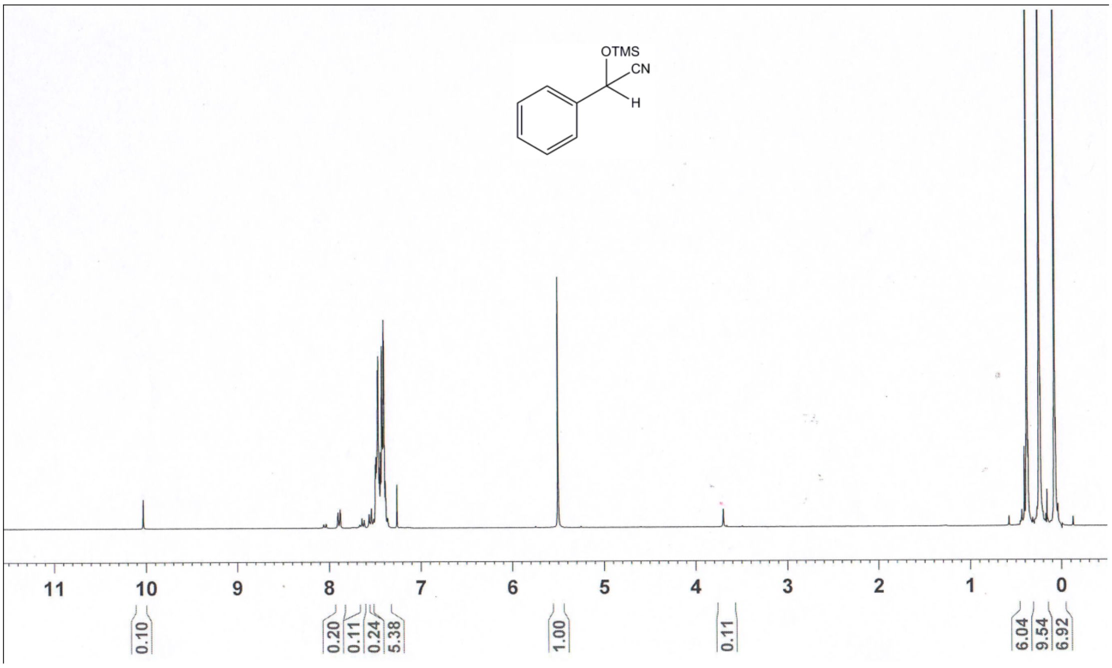

(m)[1]H NMR of crude reaction mixture corresponding to Table2, entry 3.

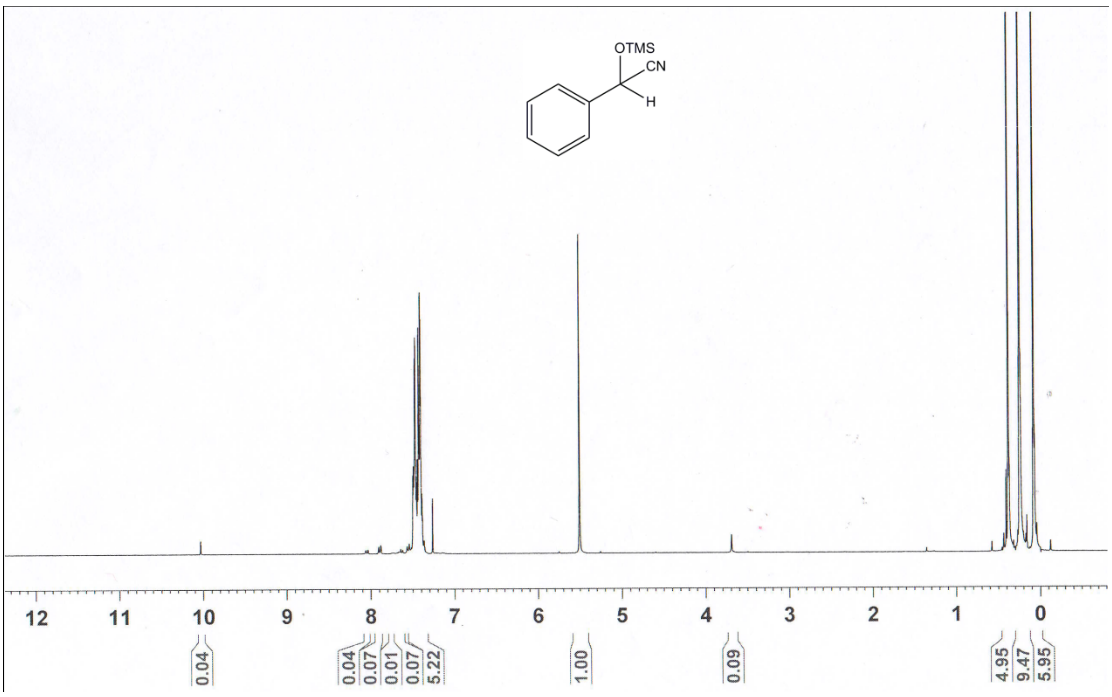

(n) [1]H NMR of crude reaction mixture corresponding to Table2, entry 4.

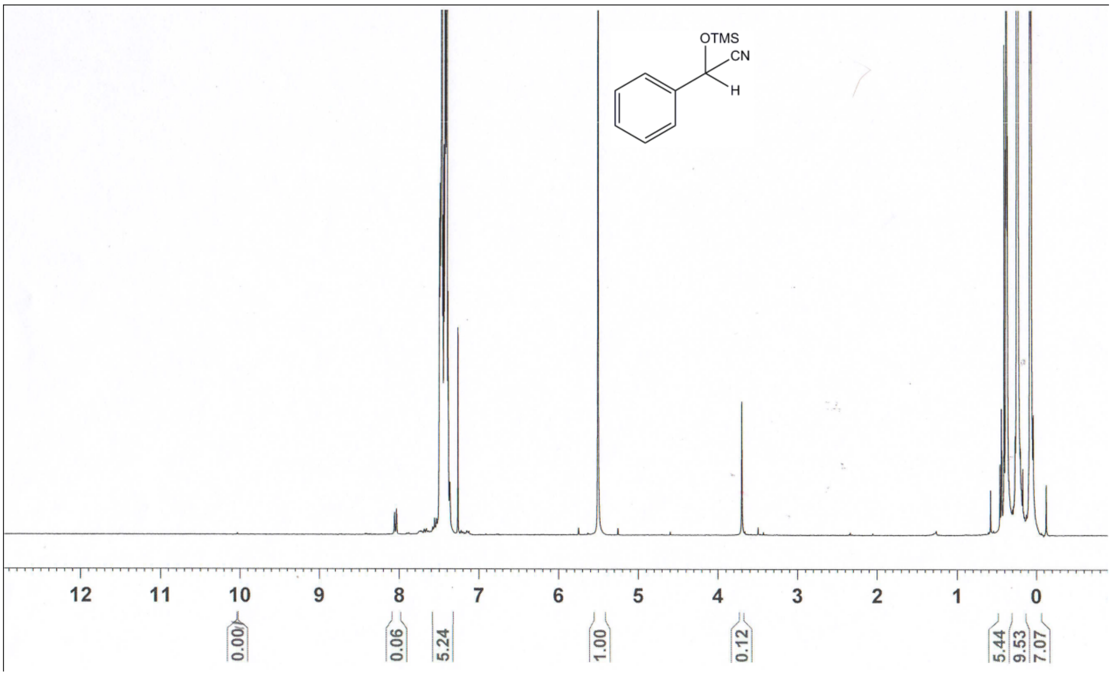

(o) ^{1}H NMR of crude reaction mixture corresponding to Table2, entry 5.

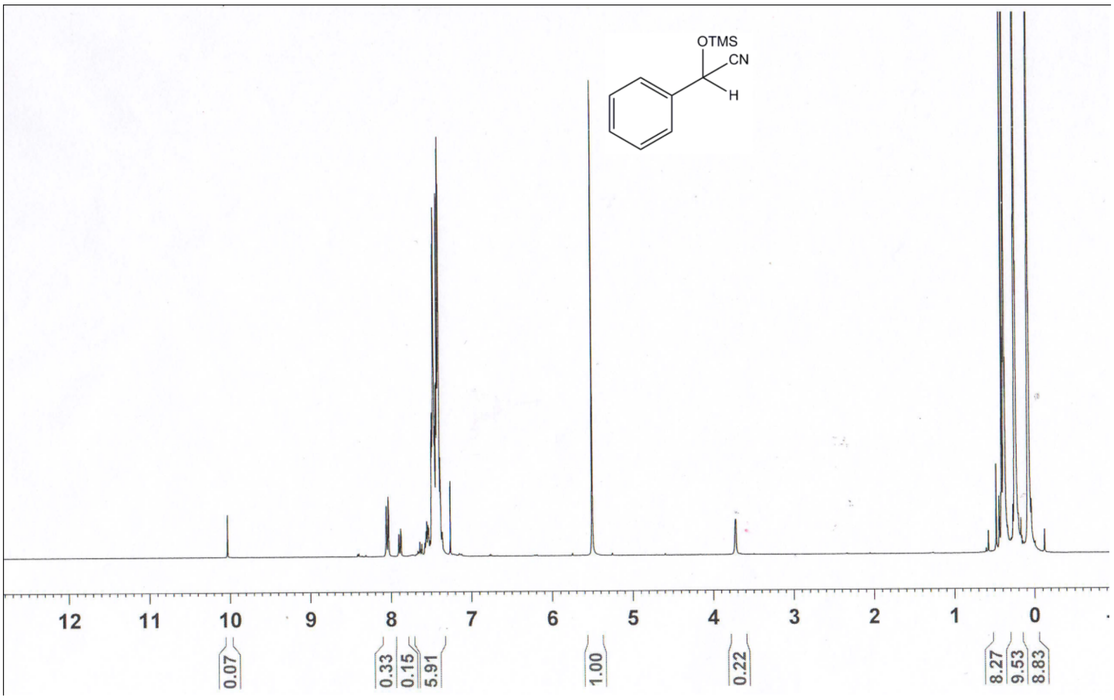

(p) ^{1}H NMR of crude reaction mixture corresponding to Table2, entry 6.

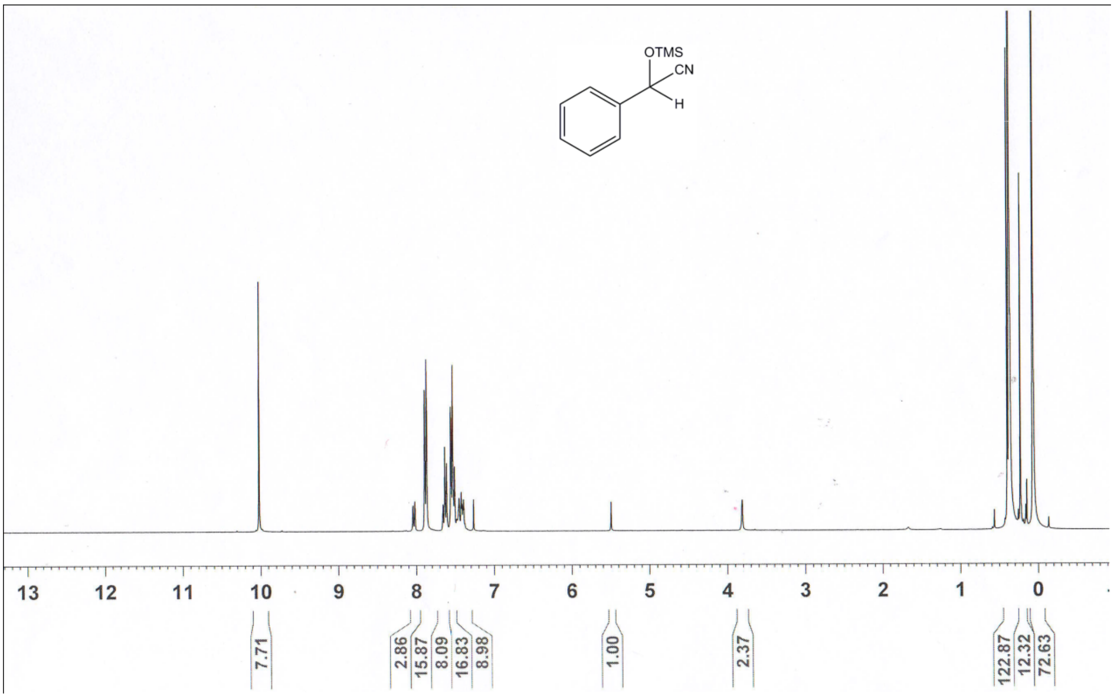

(q) [1]H NMR of crude reaction mixture corresponding to Table2, entry 7.

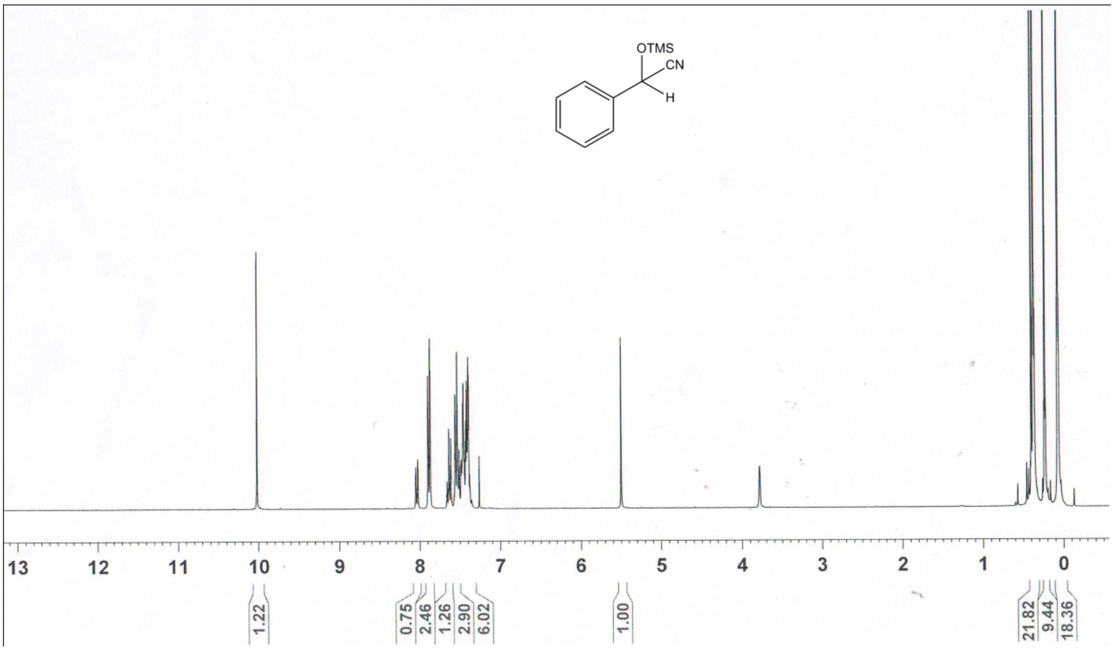

(r) [1]H NMR of crude reaction mixture corresponding to Table2, entry 8.

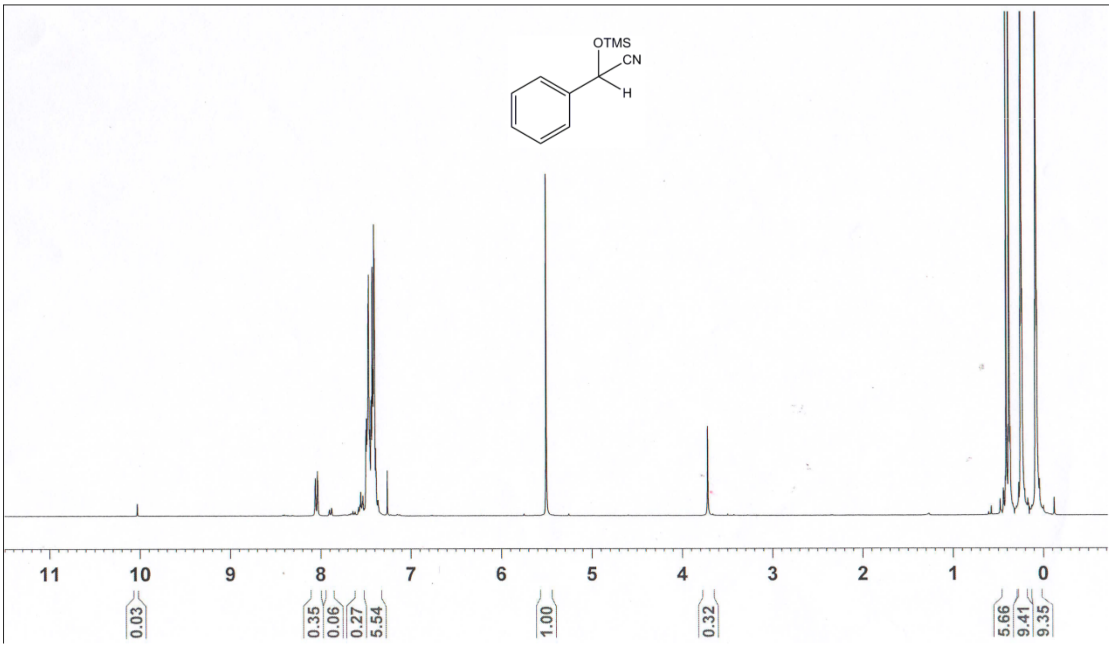

(s) ^{1}H NMR of crude reaction mixture corresponding to Table2, entry 9.

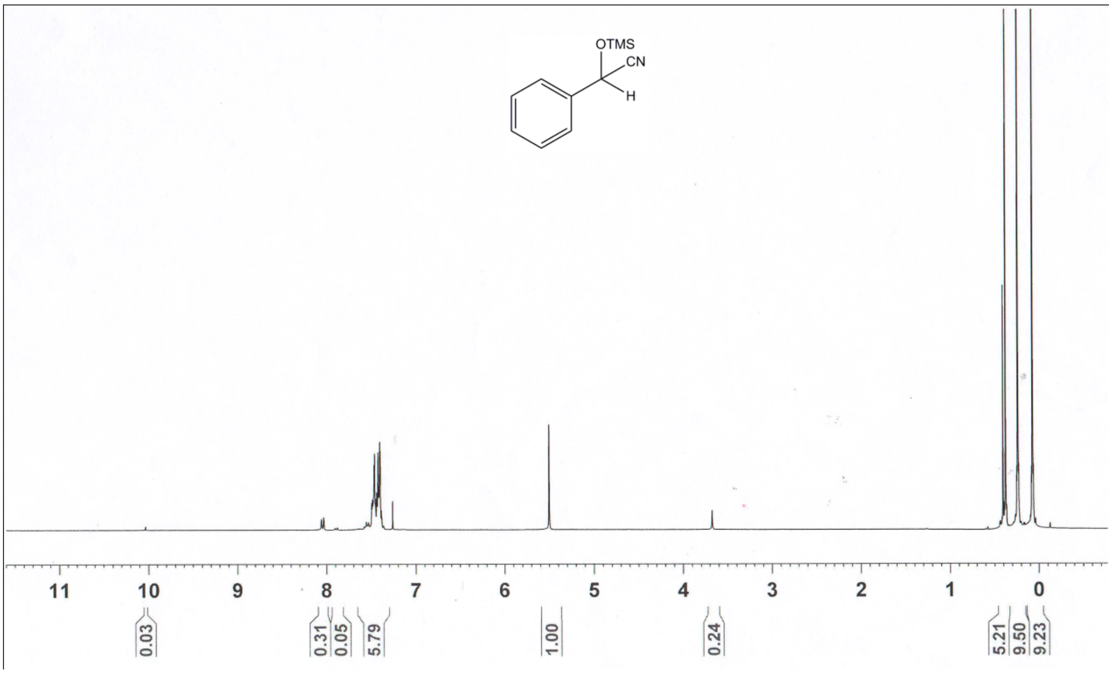

(t) ^{1}H NMR of crude reaction mixture corresponding to Table2, entry 10.

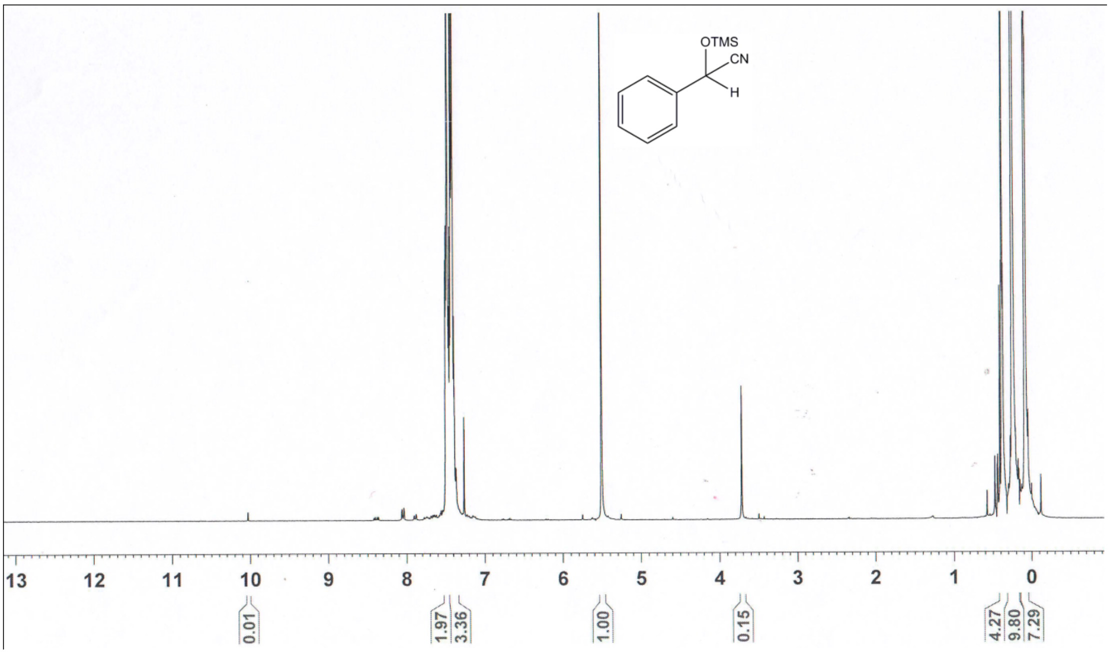

(u) ^{1}H NMR of crude reaction mixture corresponding to Table2, entry 11.

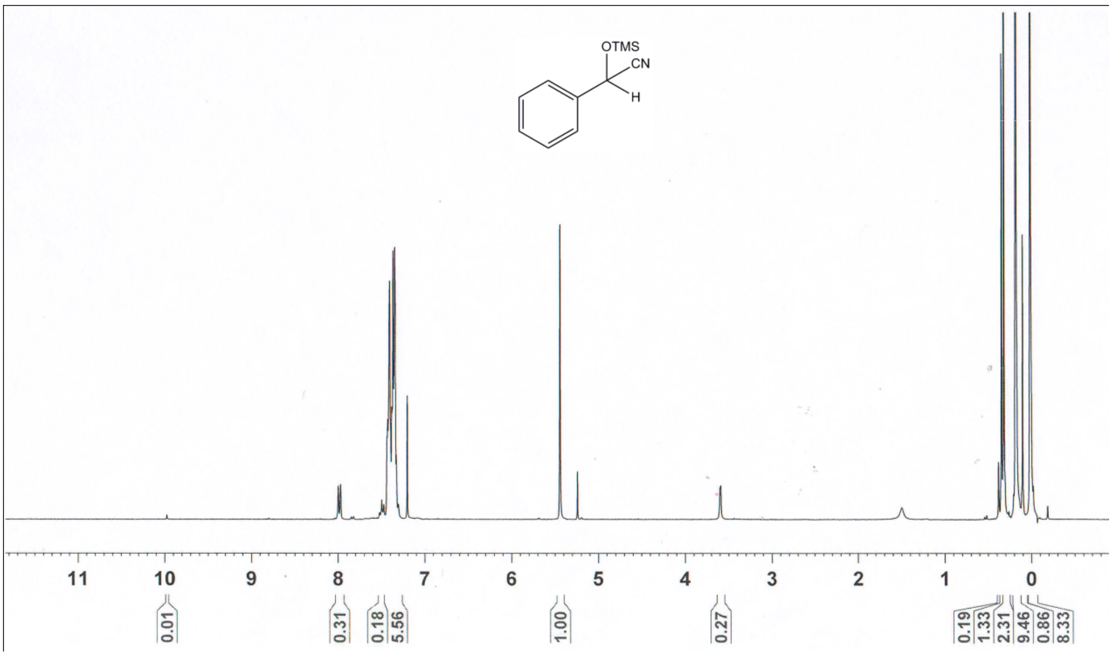

(v) ^{1}H NMR of crude reaction mixture corresponding to Table2, entry 12.

Calculation method of conversion is dividing characteristic peak area of substrate by sum of characteristic peak areas of substrate and corresponding product.

Conversion% = peak area of substrate/(peak areas of substrate +corresponding product) x 100%

5. Table S2 Comparison of the catalytic activity of MOFs in cyanosilylation reactions of benzaldehyde.

catalyst	mol % cat	molar ratio[a]	T /°C	T /h	yield (%)	TON[b]	TOF[c] /h^{-1}	ref
1	0.1	1:2	r.t.	1	56.5	565	565	this work
Sc-MOF	2	1:2	40	12	90	45	3.75	1
$[Zn_3(bpy)_{3.5}(\mu\text{-}O_2CH)_4(ClO_4)_2]_\infty$	13	1:2	r.t.	24	22	1.7	0.07	2
MIL-101(Cr)	1	1:2	40	3	98	98	33	3
CPO-27-Mn	10	1:2	40	1	100	10	10	4
Ce-MDIP1	2	1:2.4	r.t.	11	100	50	4.5	5
RPF-21-Pr	1	1:1.5	40	4	90.7	90.7	22.7	6
RPF-22-Pr	1	1:1.5	40	6	10.2	10.2	1.7	6
RPF-23-Pr	1	1:1.5	40	6	13.8	13.8	2.3	6
RPF-21-La	1	1:1.5	40	4	93.2	93.2	23.3	6
RPF-21-Nd	1	1:1.5	40	4	89.2	89.2	22.3	6
$[Fe_2Ag_2(pca)_4(pcaH)(MeOH)_2](ClO_4)_2\cdot 3MeOH$	1.7	1:2	25	3	51	30	10	7
POMOF1	1	1:2.4	r.t.	24	98.1	98.1	4	8
La-BTTc	1	1:1	r.t.	2	82	82	41	9
La-BTTc	1	1:1	r.t.	0.5	68	68	134	9
$Mn_3[(Mn_4Cl)_3(BTT)_8(CH_3OH)_{10}]_2$	11	1:2	r.t.	9	98	8.9	0.99	10
La-TTTA	2.5	1:2	r.t.	2	99.7	39.88	19.94	11
Nd-TTTA	2.5	1:2	r.t.	2	98.32	39.33	19.66	11
$Cu(BrDPMP)_2$	2	1:1.2	r.t.	2	80	40	20	12
Cu-DDQ	2.5	1:2	r.t.	1	95	38	38	13
$[Zn_3(TCPB)_2]_\infty$	2.5	1:2	r.t.	13	100	40	3.1	14
CoNiBpe 2	10	1:5	80	16	77	7.7	0.48	15
Nd(btc)-MOFs	4.5	1:2	r.t.	2	99	22	11	16
(O_2H_3)Sc-MOF	5	1:1.5	40	8	84	16.8	2.1	17
$(\mu\text{-}OH)_6$Sc-MOF	5	1:1.5	40	8.5	77.3	15.46	1.9	17
(Phen)Sc-MOF	5	1:1.5	40	7	55	11	1.6	17
RPF-18-Pr	5	1:1.5	50	3	77.8	15.56	5.2	18
RPF-18-La	5	1:1.5	50	2	85.7	17.14	8.57	18
RPF-19-Nd	5	1:1.5	50	2	94.8	18.96	9.48	18
(*R*)-1-Li	0.5	1:1	-78	0.75	97	194	258.7	19

References:

1. F. Gándara, B. Gómez-Lor, M. Iglesias, N. Snejko, E. Gutiérrez-Puebla and A. Monge, *Chem. Commun.,* 2009, 2393-2395.
2. P. Phuengphai, S. Youngme, P. Gamez and J. Reedijk, *Dalton. Trans.,* 2010, **39**, 7936-7942.
3. A. Henschel, K.Gedrich, R. Kraehnert and S. Kaskel, *Chem. Commun.,* 2008, 4192-4194.
4. H. F. Yao, Y. Yang, H. Liu, F. G. Xi and E. Q. Gao, *Journal of Molecular Catalysis A: Chemical.,* 2014, **394**, 57-65.
5. D. B. Dang, P. Y. Wu, C. He, Z. Xie and Y. C. Duan, *J. Am. Chem. Soc.,* 2010, **132**, 14321-14323.
6. R. F. D'Vries, V. A. de la Pena-O'Shea, N. Snejko, M. Iglesias, E. Gutiérrez-Puebla and M. A. Monge, *Cryst. Growth. Des.,* 2012, **12**, 5535-5545.
7. S. Nayak, K. Harms and S. Dehnen, *Inorg. Chem.,* 2011, **50**, 2714-2716.
8. Q. X. Han, X. P. Sun, J. Li, P. T. Ma and J. Y. Niu, *Inorg. Chem.,* 2014, **53**, 6107-6112.
9. T. Kajiwara, M. Higuchi and A. Yuasa, *Chem. Commun*., 2013, **49**, 10459-10461.
10. S. Horike, M. Dincă, K. Tamaki and J. R. Long, *J. Am. Chem. Soc.,* 2008, **130**, 5854-5855.
11. Y. Zhu, Y. M. Wang, J. Xu, P. Liu, H.A.B.M.D. Weththainha, Y. L. Wu, X. Q. Lu and J. M. Xie, *Journal of Solid State Chemistry.,* 2014, **219**, 259-264.
12. K. K. Raja. D. Easwaramoorthy, K. Rani, J. Rajesh, Y. Jorapurd, S. Thambidurai, PR. Athappanc and G. Rajagopala, *Journal of Molecular Catalysis A: Chemical.,* 2009, **303**, 52-59.
13. Y. Zhu, Y. M. Wang, S. Y. Zhao, P. Liu, C. Wei, Y. L. Wu, C. K. Xia and J. M. Xie, *Inorg. Chem.,* 2014, **53**, 7692-7699.
14. X. M. Lin, T. T. Li, Y. W. Wang, L. Zhang and C. Y. Su, *Chem. Asian J.,* 2012, **7**, 2796-2804.
15. R. Fernández de Luis, M. K. Urtiaga, J. L. Mesa, E. S. Larrea, M. Iglesias, T. Rojo and M. I. Arriortua, *Inorg. Chem.,* 2013, **52**, 2615-2626.
16. M. Gustafsson, A. Bartoszewicz, B. Martín-Matute, J. L. Sun, J. Grins, T. Zhao,

Z. Y. Li, G. S. Zhu and X. D. Zou, *Chem. Mater.,* 2010, **22**, 3316-3322.

17. R. F. D'Vries, V. A. de la Pena-O'Shea, N. Snejko, M. Iglesias, E. Gutiérrez-Puebla and M. A. Monge, *J. Am. Chem. Soc*., 2013, **135**, 5782-5792.
18. R. F. D'Vries, M. Iglesias, N. Snejko, E. Gutiérrez-Puebla and M. A. Monge, *Inorg. Chem.,* 2012, **51**, 11349-11355.
19. K. Mo, Y. H. Yang and Y. Cui, *J. Am. Chem. Soc.,* 2014, **136**, 1746-1749.

6. Figure S5 The comparison of 5 cycles of cyanosilylation reaction (benzaldehyde and TMSCN) with 1 as catalyst (each cycle: 0.5h).